6012 *Biochemistry* **2009,** *48,* 6012–6021
DOI: 10.1021/bi801690f

BIOCHEMISTRY
including biophysical chemistry & molecular biology
Article

A C-Truncated Glutamyl-tRNA Synthetase Specific for $tRNA^{Glu}$ Is Stimulated by Its Free Complementary Distal Domain: Mechanistic and Evolutionary Implications[†]

Daniel Y. Dubois,[‡,§] Sébastien P. Blais,[‡] Jonathan L. Huot, and Jacques Lapointe*

Regroupement québécois de Recherche sur la Fonction, la Structure et l'Ingénierie des Protéines (PROTÉO), Département de Biochimie et de Microbiologie, Université Laval, Québec, Québec, Canada G1K 7P4, [‡] D.Y.D. and S.P.B. contributed equally to this work. [§] Present address: Genizon BioSciences, Inc., 880 McCaffrey, St.-Laurent, Québec, Canada H4T 2C7

Received September 5, 2008; Revised Manuscript Received April 27, 2009

ABSTRACT: Faithful translation of the genetic code is mainly based on the specificity of tRNA aminoacylation catalyzed by aminoacyl-tRNA synthetases. These enzymes are comprised of a catalytic core and several appended domains. Bacterial glutamyl-tRNA synthetases (GluRS) contain five structural domains, the two distal ones interacting with the anticodon arm of $tRNA^{Glu}$. *Thermus thermophilus* GluRS requires the presence of $tRNA^{Glu}$ to bind ATP in the proper site for glutamate activation. In order to test the role of these two distal domains in this mechanism, we characterized the *in vitro* properties of the C-truncated *Escherichia coli* GluRSs N_{1-313} and N_{1-362}, containing domains 1−3 and 1−4, respectively, and of their N-truncated complements GluRSs $C_{314-471}$ (containing domains 4 and 5) and $C_{363-471}$ (free domain 5). These C-truncated GluRSs are soluble, aminoacylate specifically $tRNA^{Glu}$, and require the presence of $tRNA^{Glu}$ to catalyze the activation of glutamate, as does full-length $GluRS_{1-471}$. The k_{cat} of tRNA glutamylation catalyzed by N_{1-362} is about 2000-fold lower than that catalyzed by the full-length *E. coli* $GluRS_{1-471}$. The addition of free domain 5 ($C_{363-471}$) to N_{1-362} strongly stimulates this k_{cat} value, indicating that covalent connectivity between N_{1-362} and domain 5 is not required for GluRS activity; the hyperbolic relationship between domain 5 concentration and this stimulation indicates that these proteins and $tRNA^{Glu}$ form a productive complex with a K_d of about 100 μM. The K_d values of $tRNA^{Glu}$ interactions with the full-length GluRS and with the truncated GluRSs N_{1-362} and free domain 5 are 0.48, 0.11, and about 1.2 μM, respectively; no interaction was detected between these two complementary truncated GluRSs. These results suggest that in the presence of these truncated GluRSs, $tRNA^{Glu}$ is positioned for efficient aminoacylation by the two following steps: first, it interacts with GluRS N_{1-362} via its acceptor-TΨC stem loop domain and then with free domain 5 via its anticodon−Dstem−biloop domain, which appeared later during evolution. On the other hand, tRNA glutamylation catalyzed by N_{1-313} is not stimulated by its complement $C_{314-471}$, revealing the importance of the covalent connectivity between domains 3 and 4 for GluRS aminoacylation activity. The K_m values of N_{1-313} and N_{1-362} for each of their substrates are similar to those of full-length GluRS. These C-truncated GluRSs recognize only $tRNA^{Glu}$. These results confirm the modular nature of GluRS and support the model of a "recent" fusion of domains 4 and 5 to a proto-GluRS containing the catalytic domain and able to recognize its tRNA substrate(s).

To faithfully translate their genetic information into proteins, present day organisms use a set of about 20 multidomain aminoacyl-tRNA synthetases (aaRS),[1] each of them being able to specifically recognize one amino acid and a subset of "cognate" tRNA molecules and to catalyze the esterification of the former to the latter in a two-step reaction (reviewed by First (*1*)). AaRSs are divided into two classes defined by evolutionarily unrelated catalytic domains (*2*), to which were appended modules whose sizes vary from small insertions to full structural domains (reviewed by refs (*3*) and (*4*)).

For the class II alanyl-tRNA synthetase (AlaRS), characterization of various truncated forms has revealed the modular arrangement along its sequence of functional domains involved respectively in the first step (aminoacyl-AMP synthesis), the second step (aminoacyl-tRNA synthesis), and in the formation of the quaternary structure of this homotetramer (*5*). Subsequently, the 3D structure of a class I aaRS, *Escherichia coli* glutaminyl-tRNA synthetase (GlnRS) complexed with $tRNA^{Gln}$

[†]This work has been supported by Grant OGP0009597 from the Natural Sciences and Engineering Research Council of Canada (NSERC) to J.L.; J.L.H. is a doctoral fellow from the Fonds de Recherche sur la Nature et les Technologies of Québec (FQRNT).

*Address correspondence to this author. Phone: (418) 656-2131 ext 3411. Fax: (418) 656-3664. E-mail: jacques.lapointe@bcm.ulaval.ca.

[1]Abbreviations: GluRS, glutamyl-tRNA synthetase; aaRS, aminoacyl-tRNA synthetase; AlaRS, alanyl-tRNA synthetase; GlnRS, glutaminyl-tRNA synthetase; ArgRS, arginyl-tRNA synthetase; LysRS-1, class I lysyl-tRNA synthetase; GoA, glutamol adenylate; Q-base, queuosine; Glx, glutamyl and/or glutaminyl; β-ME, β-mercaptoethanol; IMAC, immobilized metal affinity chromatography; Ni-NTA, nickel−nitrilotriacetic acid; DTT, 1,3-dithiothreitol; OPD, optical path difference; SDS, sodium dodecyl sulfate; PP_i, pyrophosphate; ABD, tRNA acceptor-end-binding domain.

 Published on Web 05/18/2009 © 2009 American Chemical Society

and ATP (*6*), showed the presence of five structural domains and allowed the identification of those involved in the binding of each of these two substrates. The *in vivo* and *in vitro* characterization of GlnRS variants truncated in the tRNA acceptor-end-binding domain (ABD) demonstrated that this domain is not involved in catalysis but is important for tRNA recognition (*7*).

A small subset of class I aaRSs, those specific for glutamine (GlnRS), glutamate (GluRS), arginine (ArgRS), and lysine (LysRS-1), do not activate their amino acid substrate in the absence of their cognate tRNA (reviewed by refs (*8*) and (*9*)). In the case of *Thermus thermophilus* GluRS, comparisons of the structures of the GluRS/ATP, GluRS/ATP/Glu, GluRS/tRNA/ATP, and GluRS/tRNA/GoA complexes (where GoA is a stable analogue of glutamyl-AMP and a GluRS inhibitor) (*10*) revealed that tRNA binding to GluRS switches ATP binding to the productive mode (*11*). These 3D structures revealed the presence of five structural domains and indicated that three regions of $tRNA^{Glu}$ are likely to account for this rearrangement of the GluRS active site: the D-stem, which interacts with the stem-contact fold (SC fold) (domain 3), a region of the acceptor stem which interacts with the KISKR loop in the SC fold, and the 3′-CCA end which interacts with the loop formed by residues 43−47 in the Rossmann fold (domain 1). More recently, genes encoding small proteins homologous to one or several domains of extant aaRSs have been found, and the functions or catalytic activities of some of them have been identified (reviewed by refs (*12*−*14*)). One of them, the product of the *E. coli yadB* gene, displays 34% amino acid sequence identity with domains 1 and 2 and a part of domain 3 of *E. coli* GluRS but does not recognize $tRNA^{Glu}$ (*15*, *16*); instead, it glutamylates specifically the anticodon Q-base of $tRNA^{Asp}$ (*17*, *18*). The puzzling specificity of this GluRS paralogue for $tRNA^{Asp}$ incited us to investigate further the role of the two distal domains 4 and 5 of GluRS in the specific recognition of $tRNA^{Glu}$. For this purpose, we have constructed the C-truncated GluRSs N_{1-362} lacking domain 5, N_{1-313} lacking domains 4 and 5, and their N-truncated complements. We report here that these C-truncations markedly reduce the rate of the aminoacylation reaction, do not significantly alter the K_m for the substrates, do not alter $tRNA^{Glu}$ recognition, nor allow the mischarging of other tRNAs. Moreover, the free domain 5 ($C_{363-471}$) efficiently stimulates the aminoacylation activity of the truncated N_{1-362} lacking this domain. The significance of these results for understanding the evolution of this class I aaRS is discussed in the context of the model proposed by Siatecka et al. (*19*) for the modular evolution of the Glx-tRNA synthetase family.

MATERIALS AND METHODS

Overproduction and Purification of Full-Length and Truncated E. coli GluRSs. Genes encoding full-length and several truncated His-tagged *E. coli* GluRSs (N_{1-313}, N_{1-362}, $C_{314-471}$, and $C_{363-471}$) (Figure 1) were cloned with 5′ extensions encoding the N-terminal tag MGSSHHHHHHSSIEGR, under the control of the IPTG-inducible promoter of the pET-28c expression vector (Novagen). To facilitate the analysis of recombinant plasmids, this vector was modified as follows: the *Cla*I site in the *kan*^{r} gene was eliminated with a silent mutation, and a *Blp*I (or *Bpu*1102I) site just upstream of the T_7 terminator of the cloning region was destroyed. The inserts of recombinant plasmids with the expected restriction maps were verified by sequencing, and these plasmids were used to transform *E. coli* JP1449 (DE3)pLysS, a strain with a thermosensitive GluRS (*20*, *21*). The resulting clones were grown at 30 °C in Luria−Bertani medium (*22*), and the GluRS overproduction was triggered by adding 0.5 mM IPTG at A_{600nm} = 0.4. After induction, bacterial growth was carried out overnight at a lower temperature to prevent the formation of inclusion bodies: room temperature for the full-length GluRS and 18 °C for its truncated counterparts. Cells were then harvested by centrifugation and the pellets frozen at −80 °C.

Full-length GluRS was purified as follows: cells were thawed on ice and resuspended in 20 mM Tris-HCl (pH 7.9) containing 5 mM imidazole, lysed using chicken egg white lysozyme in the presence of the recommended concentration of "Complete, Mini, EDTA-free protease inhibitor cocktail" (Roche Diagnostics). Viscosity was reduced by incubating the lysate with DNase I on ice; then, 1 mM β-mercaptoethanol (β-ME) was added. The lysate was centrifuged for 45 min at 17500*g* at 4 °C, and the supernatant was clarified by passage through a filter with 0.22 μm pores. The enzyme was purified by immobilized metal affinity chromatography (IMAC) on a Ni-NTA agarose column (Qiagen) equilibrated in 20 mM Tris-HCl (pH 7.9) and 5 mM imidazole. The column was successively washed with this Tris buffer containing 5 and 25 mM imidazole (10 and 5 volumes, respectively). The enzyme was eluted with 1 M imidazole in the same buffer. The washing and elution buffers also contained 1 mM β-ME. The GluRS was dialyzed against 40 mM HEPES−KOH, pH 7.2, 10% glycerol, and 10 mM β-ME, concentrated with a centrifugal filter device (Amicon Ultra, Millipore), and stored at −20 °C in the storage buffer (20 mM HEPES−KOH, pH 7.2, 45% glycerol, and 5 mM β-ME).

The truncated GluRSs were purified as described above for the full-length GluRS, with the following modifications. As the yield of these truncated enzymes is lower than that of full-length GluRS, we improved the lysis by adding 0.2% Triton X-100 to

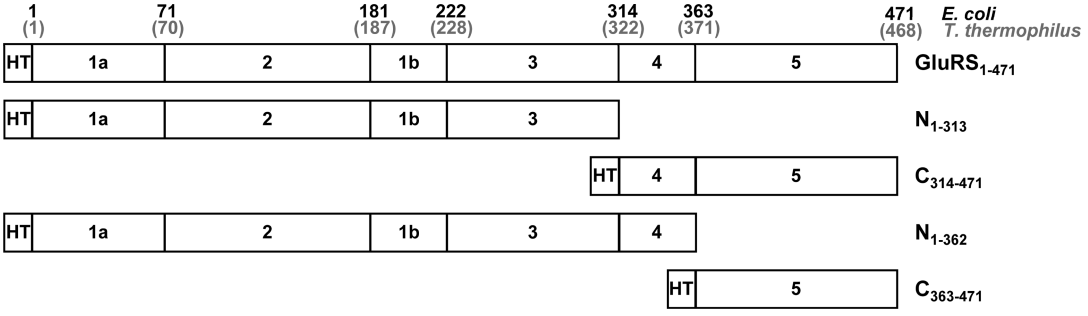

FIGURE 1: Construction of various truncated GluRSs of *E. coli*. The domain structure of *E. coli* GluRS was predicted from sequence comparison with *T. thermophilus* GluRS and its known 3-D structure. These two GluRSs have a 34% sequence identity and 58% sequence similarity. Domains are designated as follows: 1a and 1b, dinucleotide binding domain; 2, acceptor-end-binding domain; 3, stem-contact fold domain; 4 and 5, anticodon binding domains. HT is a His tag.

the lysis buffer and by using ultrasonic disruption (Virsonic digital 475, Virtis). The final elution buffer contained 500 mM imidazole. The solubility of $C_{314-471}$ was increased by the addition of 25 mM NaCl to all buffers. Prior to *in vitro* testing, His tags on $C_{314-471}$ and $C_{363-471}$ were removed as follows: the proteins were dialyzed against the digestion buffer (20 mM Tris-HCl, pH 7.9) and concentrated to 10 mg/mL. Protease factor Xa (Roche) was added in a 1 to 500 weight ratio and up to a 1 to 100 weight ratio for the digestion of N-His-tagged $C_{314-471}$. The digestion was performed at 4 °C for up to 72 h and stopped by the addition of β-ME to a final concentration of 20 mM. The digested GluRSs were then put back in the storage buffer. The free tag was eliminated during concentration on a centrifugal filter device. Earlier work with full-length GluRS showed that the presence of an N-terminal His tag did not affect its activity (Lacoste and Lapointe, unpublished results).

Overproduction and Purification of E. coli tRNA^{Glu}. *E. coli* tRNA^{Glu} was overproduced *in vivo* in *E. coli* DH5α transformed with plasmid pKR15 kindly provided by K. Rogers and D. Soll, Yale University, New Haven, CT. This plasmid was constructed by inserting into *Eco*RI−*Pst*I sites of pGF1B (*23*) the *E. coli* tRNA^{Glu} gene, where it is constitutively expressed from a synthetic promoter derived from the promoter sequence of the *E. coli* lipoprotein gene (K. Rogers and D. Soll, personal communication). The growth conditions and tRNA purification procedures were as described by Madore et al. (*24*). Unfractionated tRNA from *E. coli* MRE600 was purchased from Roche Diagnostics.

Determination of the Kinetic Parameters of Truncated GluRSs in the Aminoacylation Reaction. The aminoacylation reaction was initiated by adding the enzyme, preincubated at 37 °C, in the reaction mixtures described below. The amount of glutamyl-tRNA formed was determined by measuring the radioactivity present in 5% trichloroacetic acid precipitates of reaction mixture aliquots, as previously described (*25*). Kinetic parameters were measured in 50 mM HEPES−KOH, pH 7.2, at 37 °C with the following additional ingredients: K_m for glutamate was determined with 32 mM $MgCl_2$, 4 mM ATP, 3 mM DTT (1,3-dithiothreitol), 10 μM tRNA^{Glu} from a tRNA fraction containing 35% tRNA^{Glu}, and six different concentrations of L-[^{14}C(U)]glutamate (25 μM to 1 mM); K_m for tRNA was determined with 32 mM $MgCl_2$, 4 mM ATP, 3 mM DTT, 1 mM L-[^{14}C(U)]glutamate, and six concentrations of tRNA^{Glu} (0.5−5 μM); K_m for ATP was determined with 16 mM $MgCl_2$, 3 mM DTT, 10 μM tRNA^{Glu}, 1 mM L-[^{14}C(U)]glutamate, and six concentrations of ATP (0.1−2 mM). In each case, the six reactions were conducted simultaneously with enzyme aliquots from the same dilution. The concentrations of GluRSs (full-length or truncated) used in these assays varied from 0.62 nM to 1.4 μM and were chosen to obtain linear kinetics of glutamyl-tRNA formation during 10 min. Data were analyzed using SPSS Science's Sigma Plot 8.0 with the Enzyme Kinetics Module version 1.10. Kinetic parameter values and error estimation were calculated using a nonlinear regression based on the Michaelis−Menten equation.

Characterization of Protein−Protein Interactions. The interactions between N_{1-362} and $C_{363-471}$ were investigated by isothermal titration microcalorimetry (on a VP-ITC, MicroCal) and by white light interferometry with a nanoporous silicon biosensor (Silicon Kinetics, San Diego, CA). Interferometry experiments were conducted as described by Latterich and Corbeil (*26*). We used defined nanoporous silicon substrate coupled to reflected white light interferometry to measure refractive index changes on the porous surface. When protein is covalently coupled to the porous surface, or when protein binding to a receptor surface occurs, the change of refractive index conferred by the immobilized protein leads to a spectral shift, resulting in a wavelength shift of the spectrum. This wavelength shift, called interferogram, is a measure of protein mass bound to the surface. Specifically, incident white light is projected onto the porous silicon surface. Reflected light from the porous silicon/fluid interface and reflected light from the bulk silicon/porous silicon interface are focused onto a diffraction grating from where emitted light is measured by a photo detector. Shifts in spectral properties as a result of protein binding are computed and translated into an optical path difference (OPD) shift, which is proportional to the mass of surface-bound protein. The binding of a ligand to the receptor molecule generated an OPD shift, demonstrating that the ligand indeed bound the receptor. A carboxy polyethylene glycol 2000 chip was allowed to react during 10 min with the activation buffer (200 mM 1-ethyl-3-(3-dimethylaminopropyl)carbodiimide hydrochloride (EDC), 50 mM *N*-hydroxysulfosuccinimide diluted in the activation solution, 0.1 M MES, pH 6.0, 0.15 M NaCl), transferred in an immobilization solution (20 mM sodium acetate, pH 4.5, 1 mM EDTA) containing the $C_{363-471}$ truncated GluRS (1 μg/μL final concentration) for the sample, and containing BSA (1 μg/μL final concentration) for the reference. Then a blocking buffer (1 M ethanolamine−HCl, pH 5.0) was used during 10 min to deactivate the free succinimide esters. The "single buffer immobilization" method was used for activation. The next step was binding: the chip was equilibrated against the binding buffer (50 mM HEPES−KOH, pH 7.2, 8 mM $MgCl_2$, 1 mM β-mercaptoethanol) during 30 min; the N_{1-362} truncated GluRS was then diluted in the binding buffer at a final concentration of 100 μM, and 10 min binding was performed during which the OPD was measured.

Characterization of Protein−tRNA Interactions. The binding of the truncated GluRSs N_{1-362} and $C_{363-471}$ (domain 5) and of full-length GluRS by *E. coli* tRNA^{Glu} was investigated by analyzing the quenching of the tryptophan fluorescence of these proteins by increasing concentrations of tRNA^{Glu} in 50 mM HEPES−KOH, pH 7.2, 10 mM $MgCl_2$, and 0.1 mM dithiothreitol. The experiments were performed in triplicate. This purified tRNA^{Glu}, purchased from Sigma-Aldrich Canada Inc., has an acceptor activity of about 1070 pmol of glutamate/A_{260nm} unit. The measurements were carried out at 22 °C in a Cary Eclipse fluorescence spectrophotometer (Varian) using a 1 cm path length quartz cuvette. Excitation was done at 295 nm, and fluorescence was recorded at 340 nm, with excitation and emission bandpasses of 5 nm. We chose to measure the fluorescence for a narrow range of wavelengths because a significant amount of photobleaching took place when a fluorescence spectrum between 300 and 600 nm was recorded for each tRNA concentration. The background spectrum for the buffer and the inner filter effect (IFE) of increasing concentrations of tRNA were subtracted, and the intensity of the fluorescence was corrected for dilution due to the sequential addition of aliquots of concentrated tRNA solution. IFE was corrected for by using the equation $F_{corr} = F_{obs} \times 10^{(A_{excitation} + A_{emission})L/2}$ (*27*). This filter effect was calculated for each tRNA concentration from the A_{295nm}/A_{260nm} ratio. The path length of the 340 nm exciting beam in the solution up to the center of the quartz cell where this beam is focalized is $L/2 = 0.5$ cm (see the Cary Eclipse

Online manual and ref (*27*)); it is from this center that the fluorescence emitted in a direction perpendicular to that of the exciting beam is recorded.

The K_d values of the protein/tRNA complexes were determined by fitting the fluorescence quenching curves (F_{obs}/F_0) by nonlinear regression using the software Kaleidagraph (Synergy Software) with the following equation, where $F_{ratio} = F_{obs}/F_0$, the observed fluorescence ratio in the presence (F_{obs}) and in the absence (F_0) of ligand, Φ is the fluorescence ratio change amplitude ($1 - F^{\infty}_{ratio}$), where F^{∞}_{ratio} is F_{ratio} at an infinite concentration on ligand, P_0 is the protein concentration, K_d is the dissociation constant, and L_T is the total ligand concentration. In terms of these parameters, the degree of association is $(1 - F_{ratio})/(1 - F^{\infty}_{ratio})$ (*27*, *28*). We considered the particular case of one tRNA binding site per protein ($n = 1$ in eq II of ref (*27*)) since that stoichiometry was already established for the *E. coli* GluRS/tRNA^{Glu} complex at neutral pH (*29*, *30*).

$$F_{ratio} = 1 - \Phi\left[\frac{(K_d + P_0 + L_T) - \sqrt{(K_d + P_0 + L_T)^2 - (4P_0L_T)}}{2P_0}\right]$$

The interaction between $C_{363-471}$ and tRNA^{Glu} was also studied by retardation during electrophoresis in a polyacrylamide gel. These two macromolecules were incubated in a buffer containing 20 mM HEPES−KOH (pH 7.2), 10 mM $MgCl_2$, and 20% glycerol at 37 °C for 20 min. All samples contained 28 μM $C_{363-471}$, to which unfractionated *E. coli* tRNA containing 12% tRNA^{Glu} was added to obtain the following tRNA^{Glu} concentrations: 20, 10, 5, 2.5, and 0 μM. The samples were then submitted to electrophoresis in 5% polyacrylamide gels, as previously described (*31*), except that 25 mM Tris-HCl (pH 8.3) and 250 mM glycine were used as migration buffer. Gels were stained with Coomassie Brilliant Blue R-250. An approximate dissociation constant was measured using a simple binding isotherm and a nonlinear regression with the SigmaPlot software using eq 2 and the following terms: B = fraction of $C_{363-471}$ bound by tRNA; R_f = fraction of free receptor ($C_{363-471}$); L = ligand (unfractionated tRNA enriched with *E. coli* tRNA^{Glu}); K_d = dissociation constant.

$$B = L/(K_d + L) \quad (1)$$

Substituting B by $1 - R_f$ in eq 1, we obtain

$$R_f = 1 - L/(K_d + L) \quad (2)$$

Amino Acid Activation Assayed by ATP−PP$_i$ Exchange. Glutamate activation by full-length and C-truncated GluRSs was assayed by ATP−PP$_i$ exchange (*32*). The reactions were performed under the following conditions: 50 mM HEPES−KOH, pH 7.2, 16 mM $MgCl_2$, 2 mM ATP, 2 mM [^{32}P]pyrophosphate (PP$_i$) (1.5 Ci/mmol), 3 mM DTT, and 1 mM L-glutamate. Reactions were conducted in parallel at 37 °C either with 5 μM tRNA^{Glu} in unfractionated tRNA or without tRNA and were initiated by the addition of the enzyme preincubated at 37 °C. Aliquots of 5 μL were taken at times ranging from 1 to 45 min, and the reactions were stopped by mixing the aliquots with 10 μL of ice-cold stop mix (400 mM sodium acetate, pH 5, 0.1% SDS). From each stopped aliquot, 2 μL was spotted on a polyethyleneimine−cellulose thin-layer chromatography plate (Sigma). Separation of [^{32}P]PP$_i$ and [^{32}P]ATP was performed using as developing buffer 750 mM KH_2PO_4 (pH 3.5) and 4 M urea (*33*). The plates were dried overnight, exposed for 1 h to an imaging plate (Type BAS-IIIs, Fuji), and quantified on a Typhoon 9400 variable mode imager (Amersham Biosciences).

RESULTS

Design and Production of Two Pairs of Complementary Truncated GluRSs. The 34% identity (and 58% similarity, using Dayhoff's table) between the amino acid sequence of *E. coli* GluRS and that of *T. thermophilus* GluRS, whose 3D structure is known (*34*), did facilitate the alignment of their sequences and indicated the limits of each of the five domains of *E. coli* GluRS (Figure 1); in particular, domains 3 and 4 end at residues 313 and 362, respectively. Genes encoding N-His$_6$-tagged truncated GluRSs (see Materials and Methods) containing domains 1−3 (N_{1-313}), 1−4 (N_{1-362}), 4 and 5 ($C_{314-471}$), and domain 5 ($C_{363-471}$) were constructed and inserted into the expression vector pET-28c. To overproduce these proteins and to test their aminoacylation activity *in vivo*, these vectors were used to transform *E. coli* JP1449(DE3)pLysS whose thermosensitive GluRS does not allow cell growth above 42 °C (*20*, *21*).

Stability and in Vitro Activity of Truncated GluRSs. These truncated GluRSs were purified to homogeneity by affinity chromatography on a nickel-containing resin (Figure 2A). Incubation in the presence of factor Xa to remove the His tags

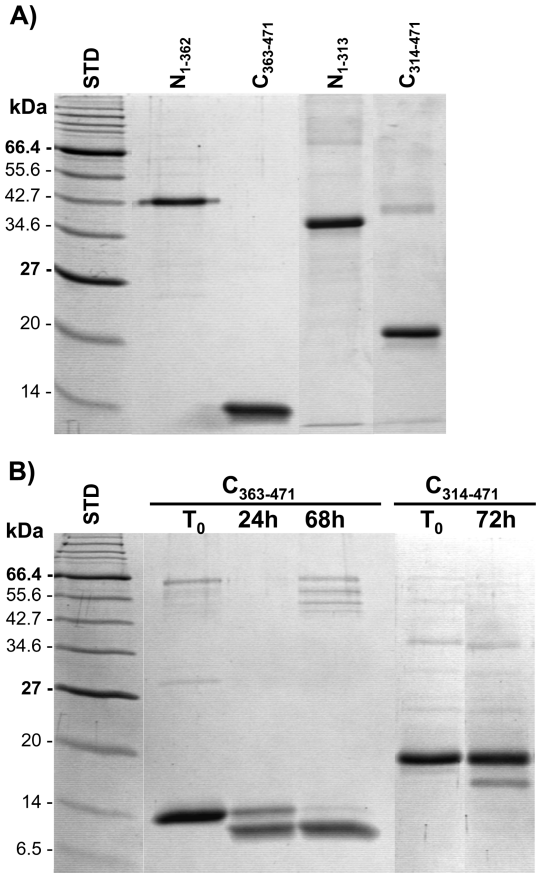

FIGURE 2: (A) SDS−PAGE analysis of overproduced His-tagged truncated GluRSs purified by affinity chromatography on Ni-NTA. The molecular weights estimated for these fragments by this method correspond to those calculated from their sequences, i.e., from left to right, respectively, 43.6, 13.8, 37.9, and 19.5 kDa. (B) His-tag removal from $C_{363-471}$ and $C_{314-471}$ by digestion with the protease factor Xa. Essentially all His tag was removed from $C_{363-471}$ after 68 h, but less than 10% of the tag of $C_{314-471}$ was removed after 72 h (last lane on the right).

Table 1: Kinetic Parameters of Full-Length and Truncated *E. coli* GluRSs in the Aminoacylation Reaction[a]

	K_m		k_{cat}			k_{cat}/K_m		
enzyme	μM	relative	s^{-1}	relative	loss		relative	loss
				Glutamate				
$GluRS_{1-471}$	130 ± 11[b]	1	3.6 ± 0.1[b]	1		2.8×10^{-2}	1	
N_{1-313}	112 ± 10	0.9	0.0083 ± 0.0002	2.3×10^{-3}	430	7.4×10^{-5}	2.7×10^{-3}	370
N_{1-362}	267 ± 48	2.1	0.0018 ± 0.0001	5.0×10^{-4}	2000	6.6×10^{-6}	2.4×10^{-4}	4200
$N_{1-362} + C_{363-471}$	158 ± 8	1.2	0.073 ± 0.001	2.1×10^{-2}	49	4.6×10^{-4}	1.7×10^{-2}	59
				ATP				
$GluRS_{1-471}$	223 ± 16	1	7.3 ± 0.1	1		3.3×10^{-2}	1	
N_{1-313}	199 ± 32	0.9	0.018 ± 0.001	2.5×10^{-3}	410	9.0×10^{-5}	2.8×10^{-3}	360
N_{1-362}	234 ± 36	1.1	0.0034 ± 0.0001	4.7×10^{-4}	2100	1.5×10^{-5}	4.5×10^{-4}	2200
$N_{1-362} + C_{363-471}$	141 ± 19	0.6	0.260 ± 0.008	3.5×10^{-2}	28	1.8×10^{-3}	5.6×10^{-2}	18
				tRNA				
$GluRS_{1-471}$	1.0 ± 0.1	1	8.0 ± 0.3	1		7.7	1	
N_{1-313}	0.7 ± 0.05	0.7	0.0210 ± 0.0004	2.6×10^{-3}	390	2.9×10^{-2}	3.7×10^{-3}	270
N_{1-362}	1.1 ± 0.2	1.1	0.0027 ± 0.0002	3.4×10^{-4}	2900	2.4×10^{-3}	3.2×10^{-4}	3100
$N_{1-362} + C_{363-471}$	16.6 ± 2.4	16.0	0.39 ± 0.05	4.9×10^{-2}	20	2.4×10^{-2}	3.1×10^{-3}	320

[a]For K_m measurements for glutamate and ATP, the concentrations of $GluRS_{1-471}$ (full-length), N_{1-313}, and N_{1-362} were 3.3 nM, 0.3 μM, and 1.4 μM, respectively. When free domain 5 ($C_{363-471}$) was added to N_{1-362}, their concentrations were 82 and 0.1 μM, respectively. For K_m measurements for $tRNA^{Glu}$, lower enzyme concentrations were used to obtain precise measurements of initial velocities: 0.6 nM $GluRS_{1-471}$, 0.18 μM N_{1-313}, 1.1 μM N_{1-362}, and 0.07 μM N_{1-362} in the presence of 82 μM $C_{363-471}$. [b]Standard deviations calculated as indicated in the Materials and Methods section.

was successful in the case of $C_{363-471}$ but inefficient for $C_{314-471}$ (Figure 2B). All of these truncated GluRSs are soluble under physiological conditions.

N_{1-313} and N_{1-362} have aminoacylation activity *in vitro*, although substantially less than full-length GluRS (Table 1), and $C_{363-471}$ or $C_{314-471}$ alone have no detectable activity. Moreover, the addition to N_{1-362} of its complement $C_{363-471}$ (domain 5) strongly stimulates its aminoacylation activity, whereas the addition to N_{1-313} of its complement $C_{314-471}$ (domains 4 and 5) has no effect when N-His-tagged $C_{314-471}$ was used or in the presence of an equimolar concentration of untagged $C_{314-471}$ from a partial digestion of N-His-tagged $C_{314-471}$ (only 10% of the truncated enzyme could be cleaved by factor Xa (Figure 2), which removes all extra N-terminal residues from domain IV).

The deletion of one or two C-terminal domains has no significant influence on the K_m for any of the three substrates (Table 1), except for the 16-fold increase in K_m for $tRNA^{Glu}$ for N_{1-362} in the presence of 82 μM free domain 5 ($C_{363-471}$). On the other hand, these deletions decrease the k_{cat} about 2000-fold for N_{1-362} and 400-fold for N_{1-313}. In the case of N_{1-362}, increasing concentrations of its complement ($C_{363-471}$) increase its k_{cat} by about 100-fold, to reach a value only about 20-fold lower than that of the full-length monomeric GluRS (Figure 3). This stimulation indicates that covalent connectivity between domain 4 and domain 5 is not a major factor for the correct positioning of the $tRNA^{Glu}$ acceptor end in the active site.

The strong decrease of the specificity constant (k_{cat}/K_m) for $tRNA^{Glu}$, essentially due to a decrease in k_{cat} (Table 1), could allow efficient competition by other tRNAs. For several aminoacyl-tRNA synthetases, discrimination against noncognate tRNAs is more often determined by kinetic effects than by binding strength (*35*, *36*) (reviewed by ref (*37*)). This possibility was tested by comparing these truncated and full-length GluRSs for the levels of glutamylation of unfractionated tRNA, and for the rates of $tRNA^{Glu}$ aminoacylation in unfractionated tRNA containing 3% $tRNA^{Glu}$, and in a fraction containing 35% $tRNA^{Glu}$ (*24*), in the presence of near-saturating concentrations of ATP and glutamate. The aminoacylation levels were identical (Figure 4), and the reduction of the rate by noncognate tRNAs was the same for intact GluRS and for N_{1-362} (Table 2), indicating that the loss of domain 5 does not allow other tRNAs to compete efficiently with $tRNA^{Glu}$ *in vitro*. Unexpectedly, N_{1-313} glutamylates tRNA at a slightly higher rate in unfractionated tRNA containing 3% $tRNA^{Glu}$. As for the full-length GluRS, these truncated GluRSs require the presence of $tRNA^{Glu}$ for glutamate activation, as shown by ATP−PP_i exchange (Figure 5). The absence of domains 4 and 5 in N_{1-313} and of

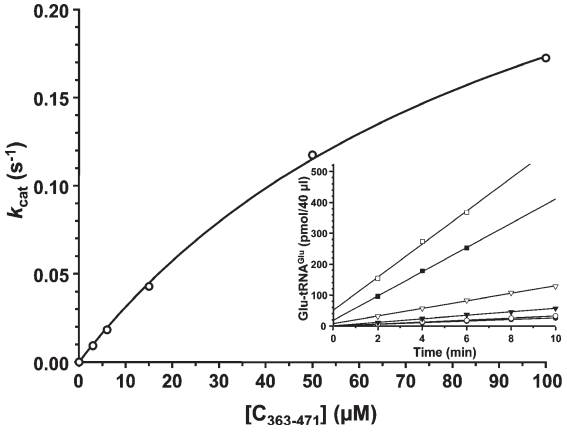

FIGURE 3: Stimulation of the N_{1-362} aminoacylation activity by increasing concentrations of $C_{363-471}$ (domain 5). As the K_m of N_{1-362} for glutamate is 267 μM (Table 1), we conducted these measurements in the presence of 1 mM L-glutamate. k_{cat} values were plotted as a function of the concentration of $C_{363-471}$ added after subtracting the value at 0 μM (0.0029 s^{-1}) from all values. The k_{cat} values were calculated from multiple-point steady-state kinetics (see insert; kinetics with 0.11 μM N_{1-362} and 0 (●), 3 (○), 6 (▼), 15 (▽), 50 (■), or 100 (□) μM $C_{363-471}$ are shown). Using the Michaelis−Menten equation, a K_d of 103 ± 8 μM is obtained. In the presence of saturating concentrations of the three substrates, k_{cat} of N_{1-362} is estimated at 0.0023 s^{-1}; in the case of K_m determinations, k_{cat} values ranged from 0.0018 to 0.0034 s^{-1} (Table 1).

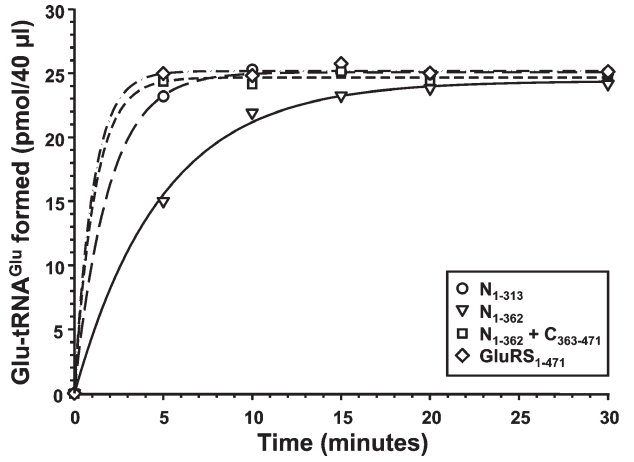

FIGURE 4: Glutamylation plateau of total unfractionated tRNA obtained with the full-length and truncated GluRSs. In this tRNA sample, $tRNA^{Glu}$ represents 3.1% of the total number of tRNA molecules.

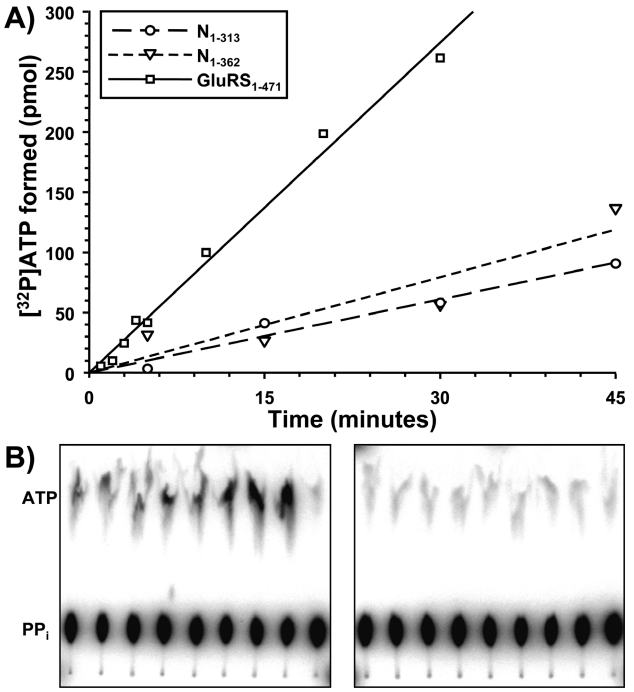

FIGURE 5: Glutamate activation by full-length $GluRS_{1-471}$ and the N_{1-313} and N_{1-362} fragments, assayed by ATP−PP_i exchange in the presence of unfractionated tRNA. The k_{cat} values for full-length GluRS, N_{1-313}, and N_{1-362} are 0.364 s^{-1}, 0.045 s^{-1}, and 0.019 s^{-1}, respectively (8-fold and 19-fold losses for N_{1-313} and N_{1-362}, respectively). In the absence of tRNA, no significant activity was detected. (A) Rate of [^{32}P]ATP formation in the presence of tRNA. (B) Thin-layer chromatograms showing the separation of [^{32}P]ATP from [^{32}P]-PP_i after reaction times of 1, 2, 3, 4, 5, 10, 20, and 30 min with $GluRS_{1-471}$ in the presence (left) and the absence (right) of $tRNA^{Glu}$. In both chromatograms, the last lane to the right is a negative control in which enzyme was omitted.

domain 5 in N_{1-362} decreases the k_{cat} of glutamate activation only 8-fold and 19-fold, respectively, compared to that of full-length GluRS (Figure 5). These losses are much lower than those observed for the aminoacylation reaction, about 400-fold and 2000-fold, respectively (Table 1).

Interactions between the C-Truncated GluRS N_{1-362}, Free Domain 5, and $tRNA^{Glu}$. Three mechanisms may explain the stimulation of the aminoacylation activity of GluRS N_{1-362} by free domain 5: (1) the formation of a transient heterodimer N_{1-362}/domain 5 more efficient than N_{1-362} to interact productively with $tRNA^{Glu}$; (2) the formation of a transient heterodimer tRNA/domain 5 more efficient than tRNA to interact productively with N_{1-362}; (3) the interaction of domain 5 with the GluRS N_{1-362}/$tRNA^{Glu}$ complex, promoting either an optimal positioning of the tRNA acceptor end in the active site or the release of the Glu-tRNA product.

To determine which one of these three mechanisms takes place, we measured the strength of the interaction in each pair of these three partners: (I) To test the existence of a $tRNA^{Glu}$/domain 5 interaction, we first analyzed the gradual disappearance of free domain 5 with increasing concentrations of $tRNA^{Glu}$ during electrophoresis in a polyacrylamide gel and obtained a K_d of about 7 μM (Figure 6A); we did not detect the tRNA/domain 5 complex on these gels probably because its subsequent dissociation and dispersion rendered it undetectable. We also measured the quenching of the fluorescence of domain 5 (which has one Trp residue) with increasing concentrations of $tRNA^{Glu}$ and found a K_d of about 1.2 μM (Figure 6B); the 7 μM value obtained by gel electrophoresis is an upper limit of the real value since there is no equilibrium between the tRNA/domain 5 complex and free tRNA and domain 5 during this experiment: the components of the complexes that dissociate during the migration have a low probability of forming new complexes. Therefore, this 7 μM value is compatible with the K_d of 1.2 μM obtained by fluorescence quenching. (II) The $tRNA^{Glu}$ interactions with N_{1-362} and with full-length GluRS were found to have K_d values of 0.11 μM and of 0.48 μM (Figure 6B), respectively, using the same fluorescence quenching method. The K_d value for full-length *E. coli* GluRS is of the same order of magnitude as those previously published for that complex by fluorescence quenching (*30*): 0.2 μM (*38*) and 0.04 μM (*39*) with differences that may be attributed to the different conditions used. The lack of inhibition of the aminoacylation activity of 2.7 nM full-length GluRS by 82 μM free domain 5 (results not shown) is consistent with the very high concentration of the covalently bound domain 5 in the vicinity of domain 4 in full-length GluRS. (III) The interaction between the complementary truncated GluRSs N_{1-362} and domain 5 was studied by three methods: quenching of the fluorescence of N_{1-362} (containing seven Trp residues) by concentrations of domain 5 (containing one Trp residue) up to 100 μM (results not shown) was consistent with a weak interaction, but the K_d value could not be determined, as it appeared to be substantially larger than 100 μM. This conclusion was also reached from the outcome of an isothermal titration microcalorimetry experiment, where no signal was obtained under conditions where an interaction with a K_d of 50 μM should have been detected. Finally, we studied the same putative protein/protein interaction by white light interferometry with a nanoporous silicon biosensor (*26*) to which domain 5 had been covalently linked (see Materials and Methods). The flow of 100 μM N_{1-362} above this layer of domain 5 gave the same OPD change as in the control reaction, when it flowed above a layer of covalently linked bovine serum albumin (Figure 7). These results are consistent with these protein fragments having no interaction in the absence of $tRNA^{Glu}$. The corresponding K_d for such an interaction would be much higher than 100 μM and therefore not in the range of physiologically significant protein/protein interactions (*40*).

DISCUSSION

The stability and solubility of the four truncated forms of *E. coli* GluRS described here (Figure 2) show that the positions of

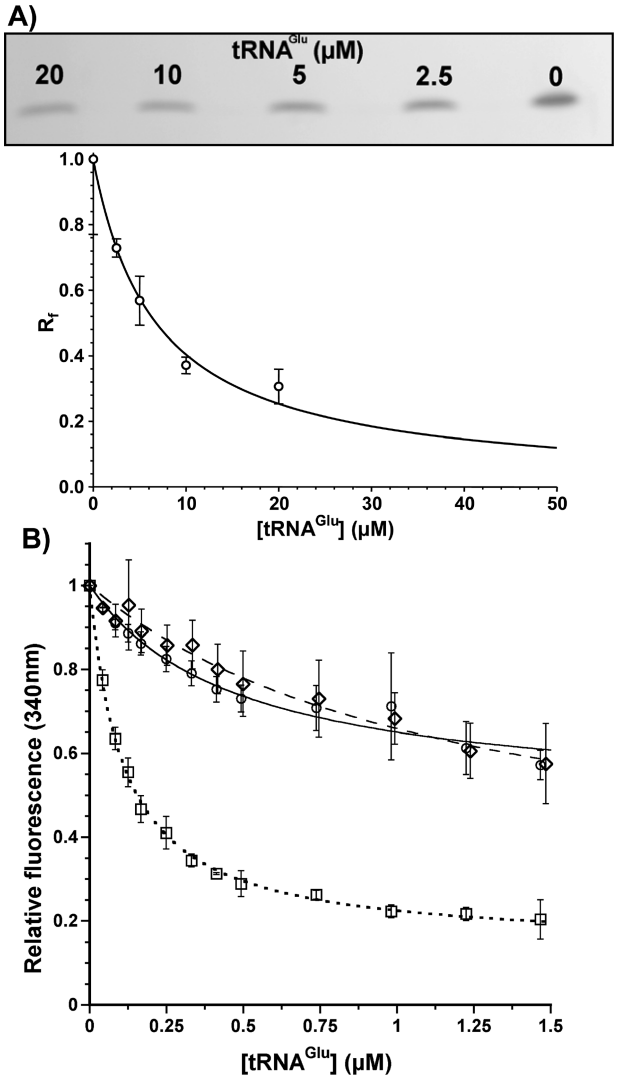

FIGURE 6: Interactions of tRNA^{Glu} with the truncated GluRSs $C_{363-471}$ (domain 5) and N_{1-362}. (A) Detection of the binding of GluRS $C_{363-471}$ to tRNA^{Glu} by electrophoresis on polyacrylamide gel under nondenaturing conditions. All lanes contained 28 μM $C_{363-471}$ and, from left to right, 20, 10, 5, 2.5, and 0 μM *E. coli* tRNA^{Glu}. Both free tRNA and free domain 5 remained in the migration front shown here. The tRNA−protein complex was too diffuse to be detected with the stain used (Coomassie Brilliant Blue), but the disappearance of $C_{363-471}$ from the migration front was quantified on three separate gels, allowing us to estimate a K_d of 7 ± 1 μM (for the procedure, see the Materials and Methods section). (B) Measurements of the K_d values of the complexes of tRNA^{Glu} with the truncated GluRSs $C_{363-471}$ and N_{1-362} and with full-length $GluRS_{1-471}$ by fluorescence spectrophotometry (see Materials and Methods). Increasing concentrations of tRNA^{Glu} were added to protein solution containing 0.2 μM $GluRS_{1-471}$ (○), or 0.25 μM N_{1-362} (□), or 1.4 μM of $C_{363-471}$ (◇). The intensity of the fluorescence was recorded after each addition of tRNA (see Materials and Methods), and the corrected relative fluorescence (see Materials and Methods) was plotted as a function of the tRNA^{Glu} concentration. Tests were done in triplicate. The following K_d were calculated by nonlinear regression (see Materials and Methods): $GluRS_{1-471}$, 0.48 ± 0.09 μM; N_{1-362}, 0.11 ± 0.004 μM; $C_{363-471}$, 1.2 ± 0.25 μM.

hinges between domains 3 and 4 and between domains 4 and 5 in *E. coli* GluRS were identified correctly by comparison with the known 3D structure of *T. thermophilus* GluRS (Figure 1). Despite the low k_{cat} values in the aminoacylation reaction of the fragments N_{1-313} and N_{1-362}, which contain the catalytic site, the facts that their K_m values for glutamate, ATP, and tRNA^{Glu} in the aminoacylation reaction are nearly identical to those of the

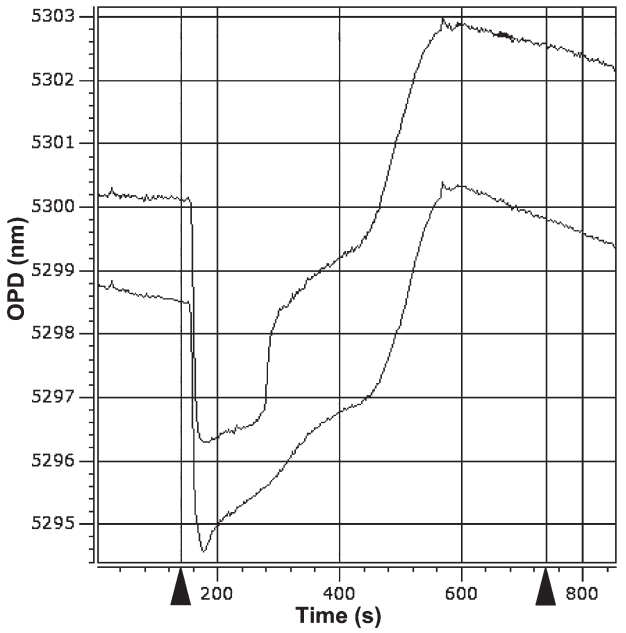

FIGURE 7: Attempts at detecting an interaction between the complementary truncated GluRSs N_{1-362} and $C_{363-471}$ (free domain 5) by white light interferometry with a nanoporous silicon biosensor (see Materials and Methods). The $C_{363-471}$ truncated GluRS and a bovine serum albumin reference were immobilized in separate channels on a carboxy polyethylene glycol 2000 chip at a final concentration of 1 μg/μL each (see Materials and Methods section). For 10 min, N_{1-362} was injected into both channels at a concentration of 100 μM, and the resulting shift in OPD was measured. Subtraction of the sample channel ($C_{363-471}$, lower curve) from the reference channel (BSA, upper curve) for the time frame indicated by the arrows on the *x*-axis revealed no significant increase in ligand binding for the channel containing immobilized $C_{363-471}$.

Table 2: Estimated k_{cat} Values for tRNA Aminoacylation by C-Truncated GluRSs[a]

	k_{cat} (s^{-1})	
enzyme	unfractionated tRNA	tRNA^{Glu} enriched
$GluRS_{1-471}$	2.52	2.93
N_{1-313}	1.01×10^{-2}	0.74×10^{-2}
N_{1-362}	0.87×10^{-3}	1.01×10^{-3}

[a]These values were obtained in the presence of 4 μM tRNA^{Glu} present in unfractionated tRNA (containing 3% tRNA^{Glu}) from *E. coli* and of a tRNA^{Glu}-enriched fraction (containing 35% tRNA^{Glu}) from the overproducing strain *E. coli* DH5α/pKR15. These values were obtained from the initial velocity of the aminoacylation reaction in the presence of saturating concentrations of the three substrates (see Materials and Methods). The standard deviations of these velocity values are of less than 2%.

full-length GluRS (Table 1), that they are specific for tRNA^{Glu} (Figure 4 and Table 2), and that they require tRNA to activate glutamate (Figure 5) indicate that their structures are identical to those of the corresponding parts in full-length GluRS. The conservation of these properties indicates that domains 4 and 5, which interact with the tRNA anticodon arm (*41*), increase the k_{cat} value either by fostering the correct orientation of the tRNA acceptor end in the active site or by facilitating the release of Glu-tRNA.

Both N_{1-313} and N_{1-362} contain domain 2, the tRNA acceptor-end-binding domain (ABD) which is inserted into domain 1, and the Rossmann fold which includes the active site (Figure 1). The ABD of *E. coli* GluRS contains a zinc finger (*42*) which modulates glutamate binding via the tRNA acceptor arm (*38*);

the identity of the K_m values for glutamate of these truncated GluRSs and of full-length GluRS reveals that this ABD does not require the presence of the distal domains 4 and 5 to fulfill this function. Considering that this ABD domain is part of the core enzyme (*43*) which corresponds to the putative ancestral minimalist GluRS, it is likely that the affinity of the ancestral GluRS for glutamate was modulated by its interaction with its minimalist tRNA substrate, possibly a single stem and loop domain corresponding to the acceptor-TΨC stem loop of present day tRNAs. The requirement of the truncated N_{1-313} and N_{1-362} for tRNA in the glutamate activation reaction suggests that this property was present in the ancestral minimalist GluRS.

The stimulation of the aminoacylation activity of the N_{1-362} fragment (GluRS lacking its C-terminal domain 5) by increasing concentrations of its complementary domain 5 (Figure 3) indicates a K_d value of about 100 μM. The strength of this stimulation cannot be attributed to a single interaction, as it occurs in the aminoacylation reaction mixture where tRNA and these two complementary truncated GluRSs are present; three interactions may contribute to this stimulation: those between N_{1-362} and domain 5 (Figure 6B), between tRNA and domain 5 (Figure 6A), and between N_{1-362} and tRNA (Figure 6B). Considering that the K_d values of the $tRNA^{Glu}$/domain 5 and $tRNA^{Glu}$/ N_{1-362} interactions are about 1.2 μM and 0.11 μM, respectively (Figure 6), the relative strengths of these interactions and the absence of significant interaction between the complementary truncated GluRSs N_{1-362} and domain 5 (Figure 7) suggest that, in the aminoacylation reaction catalyzed in the presence of these two proteins, the first interaction is between GluRSs N_{1-362} and the acceptor-TΨC stem loop domain of $tRNA^{Glu}$, and that free domain 5 then interacts with the evolutionary more recent part of $tRNA^{Glu}$; its anticodon−Dstem−biloop domain. The fact that the apparent K_m of N_{1-362} for tRNA in the presence of 82 μM domain 5 is 16-fold higher than in its absence (16.6 versus 1.1 μM; see Table 1) is probably due to the titration of $tRNA^{Glu}$ by free domain 5, if we suppose that a productive interaction between free domain 5 and $tRNA^{Glu}$ takes place only in a complex of GluRS N_{1-362} and $tRNA^{Glu}$.

The lack of significant interaction between GluRSs N_{1-362} and free domain 5 in *E. coli* GluRS (Figure 7) is consistent with the high mobility (8° rotation) of domain 5 relative to domain 4 of *T. thermophilus* GluRS, without changing their folds, revealed by the crystallographic structures of this enzyme in the presence and in the absence of its $tRNA^{Glu}$ substrate (*11*). The flexibility of the hinge linking domains 4 and 5 is probably important for GluRS activity. In the evolutionarily related GlnRS, the anticodon-binding C-terminal β-barrels are mobile both in the ligand-free enzyme and in the GlnRS/$tRNA^{Gln}$ complex (ref (*44*) and references therein); this mobility might have the same function in GlnRS as the mobility of domain 5 with respect to its complement (domains 1−4) in GluRS, whatever this function is.

For both *E. coli* GluRS and GlnRS, the anticodon and the acceptor stem/discriminator base domains are strong determinants of their tRNA substrate recognition (reviewed by Sherman et al. (*45*), Ibba et al. (*46*), and Giegé and Frugier (*47*)). Several mutations or modifications that affect the interaction of these aaRSs with their cognate tRNA at positions remote from the active site often result in significant effects on the activity (reviewed by Ibba et al. (*46*) and Giegé and Lapointe (*48*)), revealing functional connectivity during substrate recognition. In *E. coli* GlnRS, two potential connectivity subdomains have been identified, based on structural and genetic studies (reviewed by Sherman et al. (*45*)): (1) a loop−β-strand−α-helix motif whose N-terminal end residues Gln318 and Lys317 interact with the inside of the L-shaped tRNA and with Gln234 in the acceptor-binding domain, respectively, and whose C-terminal end residue Arg341 is essential for the specific recognition of the anticodon base U34 (*49*); (2) a motif inserted at the junction of the proximal and distal anticodon-binding β-barrels and made of the two antiparallel β-strands β-20 and β-21 (*44*, *50*) connected by an extended loop (residues 476−492) which packs against the active site. Moreover, this connectivity is also mediated by the intact structure of tRNA, as evidenced by the fact that an anticodon stem−loop microhelix did not enhance aminoacylation of the acceptor stem microhelix (*51*). As the two C-terminal domains of *E. coli* GluRS and GlnRS are structurally and topologically very different (two α-helical domains in GluRS (*34*) and two β-barrels in GlnRS (*6*)), they cannot be linked evolutionarily, and thus the mechanisms for their connectivity with their respective active site domains must be different.

In a class II aaRS, *T. thermophilus* ProRS, a hinge movement of the anticodon-binding domain in relation to the catalytic domain was also observed following $tRNA^{Pro}$ binding (*52*) (reviewed by ref (*37*)). Such conformational flexibility, including subdomain rotation, was shown to be important for the catalytic activity of the dihydrofolate reductase (*53*) (reviewed by ref (*54*)).

The flexibility between domains 4 and 5 of *E. coli* GluRS may influence the rate-limiting step of the aminoacylation reaction. In the ternary system that we have studied, a weak interaction between C_{1-362} and free domain 5 may be mediated in their individual, relatively much stronger interactions with distinct parts of $tRNA^{Glu}$. If we assume that the rate of association (k_{on}) between these domains is diffusion controlled, and if we take for this rate the basal k_{on} value of 10^5 s^{-1} M^{-1} obtained for the association between several couples of macromolecules in the absence of electrostatic effects (*55*), the apparent K_d of 10^{-4} M obtained for the stimulation of $tRNA^{Glu}$ aminoacylation in the presence of C_{1-362} and free domain 5 (Figure 3) means that the rate of dissociation k_{off} between these domains is of the order of 10 s^{-1} ($k_{off} = K_d k_{on} = 10^{-4}$ M × 10^5 s^{-1} M^{-1}), a value similar to the rate-limiting step of the aminoacylation reaction catalyzed by full-length GluRS (reviewed by ref (*56*)). This model could be tested by characterizing GluRS variants altered in residues involved in the interaction between these domains, in particular, in residues of the hinge linking these domains.

The importance of the integrity of the stem-contact (SC) fold for communication between the N-terminal active site domain of *E. coli* cysteinyl-tRNA synthetase and its C-terminal domains was revealed by the lack of stimulation of the weak aminoacylation activity of the former by the latter for fragments ending within the SC fold (*13*). This region, initially considered as an extension of the Rossmann fold in *T. thermophilus* GluRS (*34*), was later found to be a distinct domain in the high-resolution structure of *T. thermophilus* methionyl-tRNA synthetase and was identified in all class I aaRSs that are active as monomers (i.e., those specific for M, I, V, L, C, R, E, and Q) (*57*). It directly connects the Rossmann fold with the C-terminal anticodon-binding domains and docks with the inner side of the L-shaped tRNA. In the present work, we show that efficient glutamylation of $tRNA^{Glu}$ by *E. coli* GluRS requires covalent connectivity between the stem-contact (SC) fold and the distal domain(s), as indicated by the lack of stimulation by the $C_{314-471}$ fragment, of the weak aminoacylation activity of its complementary fragment N_{1-313} (see above). On the other hand, covalent connectivity

between the two C-terminal domains of GluRS, involved in tRNA anticodon arm binding, is not essential for efficient glutamylation of $tRNA^{Glu}$, as shown by the strong stimulation of the aminoacylation activity of the N_{1-362} fragment by saturating concentrations of its complementary fragment $C_{363-471}$ (Table 1 and Figure 3).

The capacity of several aaRSs to aminoacylate specifically RNA minihelices or microhelices that recapitulate the acceptor stems of their cognate tRNAs led to the model (*43*) of primordial aaRSs composed of a conserved domain with its active site for adenylate synthesis and transfer of the activated amino acid to a tRNA ancestor containing only the acceptor-TΨC stem−loop domain. The fact that the C-truncated GluRS N_{1-313} and N_{1-362} have a significant level of aminoacylation activity specific for $tRNA^{Glu}$ supports the model of GlxRS evolution by addition of an anticodon-binding domain to an ancestral domain containing the active site (*19*). Moreover, the strong stimulation of the aminoacylation activity of GluRS N_{1-362} by the highly soluble free domain 5 (Figure 3) suggests that the ancestral GluRS has evolutionarily picked up this domain first noncovalently as a step to covalent attachment; in the early bacteria where such an event might have taken place, the small increase in protein biosynthesis efficiency may have contributed to the selection of a recombination event joining their genes.

The rates of the tRNA-dependent glutamate activation reaction catalyzed by the C-truncated GluRS N_{1-313} and GluRS N_{1-362} are only 8-fold and 19-fold lower than that of full-length GluRS, respectively (Figure 5), compared to about 400-fold and 2000-fold, respectively, for the aminoacylation reaction (Table 1); these results suggest that the active site elements participating to glutamate activation in the putative proto-GluRS were similar to those of extant GluRSs and that the addition of domains 4 and 5 improved mostly the rate of the transfer reaction or by facilitating the release of Glu-tRNA.

ACKNOWLEDGMENT

The authors thank Dr. Jacques Corbeil and Dr. Ian de Belle (Centre de Recherche, Pavillon CHUL, Université Laval) for the protein−protein interaction studies by interferometry, Mrs. Rodica Neagu Plesu (Département de Chimie et Centre de Recherche sur les Matériaux Avancés (CERMA), Université Laval) for advice about the use of the Varian Cary Eclipse fluorescence spectrofluorometer, Mrs. Caroline Cormier and Mr. Olivier Valade for early work on the truncated GluRSs, and the unidentified reviewers for their constructive comments.

REFERENCES

(1) First, E. A. (2005) Catalysis of the tRNA aminoacylation reaction, in The Aminoacyl-tRNA Synthetases (Ibba, M., Francklyn, C., and Cusack, S., Eds.) pp 328−352, Eurekah.com/Landes Bioscience, Georgetown, TX.

(2) Eriani, G., Delarue, M., Poch, O., Gangloff, J., and Moras, D. (1990) Partition of tRNA synthetases into two classes based on mutually exclusive sets of sequence motifs. *Nature 347*, 203–206.

(3) Ibba, M., and Soll, D. (2000) Aminoacyl-tRNA synthesis. *Annu. Rev. Biochem. 69*, 617–650.

(4) Ribas de Pouplana, L., and Schimmel, P. (2001) Two classes of tRNA synthetases suggested by sterically compatible dockings on tRNA acceptor stem. *Cell 104*, 191–193.

(5) Jasin, M., Regan, L., and Schimmel, P. (1983) Modular arrangement of functional domains along the sequence of an aminoacyl tRNA synthetase. *Nature 306*, 441–447.

(6) Rould, M. A., Perona, J. J., Soll, D., and Steitz, T. A. (1989) Structure of *E. coli* glutaminyl-tRNA synthetase complexed with $tRNA^{Gln}$ and ATP at 2.8 Å resolution. *Science 246*, 1135–1142.

(7) Schwob, E., and Soll, D. (1993) Selection of a "minimal" glutaminyl-tRNA synthetase and the evolution of class I synthetases. *EMBO J. 12*, 5201–5208.

(8) Meinnel, T., Mechulam, Y., and Blanquet, S. (1995) Aminoacyl-tRNA synthetases: Occurence, structure, and function, in tRNA: Structure, Biosynthesis, and Function (Soll, D., and RajBhandary, U. L., Eds.) pp 251−292, American Society for Microbiology, Washington, DC.

(9) Ibba, M., Losey, H. C., Kawarabayasi, Y., Kikuchi, H., Bunjun, S., and Soll, D. (1999) Substrate recognition by class I lysyl-tRNA synthetases: a molecular basis for gene displacement. *Proc. Natl. Acad. Sci. U.S.A. 96*, 418–423.

(10) Desjardins, M., Garneau, S., Desgagnés, J., Lacoste, L., Yang, F., Lapointe, J., and Chênevert, R. (1998) Glutamyl adenylate analogues are inhibitors of glutamyl-tRNA synthetase. *Bioorg. Chem. 26*, 1–13.

(11) Sekine, S.-i., Nureki, O., Dubois, D. Y., Bernier, S., Chênevert, R., Lapointe, J., Vassylyev, D. G., and Yokoyama, S. (2003) ATP binding by glutamyl-tRNA synthetase is switched to the productive mode by tRNA binding. *EMBO J. 22*, 676–688.

(12) Ibba, M., and Soll, D. (2004) Aminoacyl-tRNAs: setting the limits of the genetic code. *Genes Dev. 18*, 731–738.

(13) Zhang, C. M., and Hou, Y. M. (2005) Domain-domain communication for tRNA aminoacylation: the importance of covalent connectivity. *Biochemistry 44*, 7240–7249.

(14) Francklyn, C. (2005) tRNA synthetase-like proteins, in The Aminoacyl-tRNA Synthetases (Ibba, M., Francklyn, C., and Cusack, S., Eds.) pp 285−297, Eurekah.com/Landes Bioscience, Georgetown, TX.

(15) Dubois, D. Y., Blaise, M., Becker, H. D., Campanacci, V., Keith, G., Giegé, R., Cambillau, C., Lapointe, J., and Kern, D. (2004) An aminoacyl-tRNA synthetase-like protein encoded by the *Escherichia coli yadB* gene glutamylates specifically $tRNA^{Asp}$. *Proc. Natl. Acad. Sci. U.S.A. 101*, 7530–7535.

(16) Campanacci, V., Dubois, D. Y., Becker, H. D., Kern, D., Spinelli, S., Valencia, C., Pagot, F., Salomoni, A., Grisel, S., Vincentelli, R., Bignon, C., Lapointe, J., Giegé, R., and Cambillau, C. (2004) The *Escherichia coli* YadB gene product reveals a novel aminoacyl-tRNA synthetase like activity. *J. Mol. Biol. 337*, 273–283.

(17) Salazar, J. C., Ambrogelly, A., Crain, P. F., McCloskey, J. A., and Soll, D. (2004) A truncated aminoacyl-tRNA synthetase modifies RNA. *Proc. Natl. Acad. Sci. U.S.A. 101*, 7536–7541.

(18) Blaise, M., Becker, H. D., Keith, G., Cambillau, C., Lapointe, J., Giegé, R., and Kern, D. (2004) A minimalist glutamyl-tRNA synthetase dedicated to aminoacylation of the $tRNA^{Asp}$ QUC anticodon. *Nucleic Acids Res. 32*, 2768–2775.

(19) Siatecka, M., Rozek, M., Barciszewski, J., and Mirande, M. (1998) Modular evolution of the Glx-tRNA synthetase family—Rooting of the evolutionary tree between the bacteria and archaea/eukarya branches. *Eur. J. Biochem. 256*, 80–87.

(20) Russell, R. R. B., and Pittard, A. J. (1971) Mutants of *Escherichia coli* unable to make protein at 42°C. *J. Bacteriol. 108*, 790–798.

(21) Lapointe, J., and Delcuve, G. (1975) Thermosensitive mutants of *Escherichia coli* K-12 altered in the catalytic subunit and in a regulatory factor of the glutamy-transfer ribonucleic acid synthetase. *J. Bacteriol. 122*, 352–358.

(22) Sambrook, J., Fritsch, E. F., and Maniatis, T. (1989) Molecular cloning: a laboratory manual , 2nd ed., Cold Spring Harbor Laboratory, Cold Spring Harbor, NY.

(23) Normanly, J., Masson, J. M., Kleina, L. G., Abelson, J., and Miller, J. H. (1986) Construction of two *Escherichia coli* amber suppressor genes: $tRNA^{Phe}_{CUA}$ and $tRNA^{Cys}_{CUA}$. *Proc. Natl. Acad. Sci. U.S.A. 83*, 6548–6552.

(24) Madore, E., Florentz, C., Giegé, R., Sekine, S., Yokoyama, S., and Lapointe, J. (1999) Effect of modified nucleotides on *Escherichia coli* $tRNA^{Glu}$ structure and on its aminoacylation by glutamyl-tRNA synthetase. Predominant and distinct roles of the mnm^5 and s^2 modifications of U34. *Eur. J. Biochem. 266*, 1128–1135.

(25) Lapointe, J., Levasseur, S., and Kern, D. (1985) Glutamyl-tRNA synthetase from *Escherichia coli*. *Methods Enzymol. 113*, 42–49.

(26) Latterich, M., and Corbeil, J. (2008) Label-free detection of biomolecular interactions in real time with a nano-porous silicon-based detection method. *Proteome Sci. 6*.

(27) Roy, S. (2004) Fluorescence quenching methods to study protein-nucleic acid interactions. *Methods Enzymol. 379*, 175–187.

(28) Lam, S. S., and Schimmel, P. R. (1975) Equilibrium measurements of cognate and noncognate interactions between aminoacyl transfer RNA synthetases and transfer RNA. *Biochemistry 14*, 2775–2780.

(29) Kern, D., and Lapointe, J. (1979) Glutamyl transfer ribonucleic acid synthetase of *Escherichia coli*. Study of the interactions with its substrates. *Biochemistry 18*, 5809–5818.

(30) Willick, G. E., and Kay, C. M. (1976) Circular dichroism study of the interaction of glutamyl-tRNA synthetase with $tRNA^{Glu2}$. *Biochemistry 15*, 4347–4352.
(31) Oshikane, H., Sheppard, K., Fukai, S., Nakamura, Y., Ishitani, R., Numata, T., Sherrer, R. L., Feng, L., Schmitt, E., Panvert, M., Blanquet, S., Mechulam, Y., Soll, D., and Nureki, O. (2006) Structural basis of RNA-dependent recruitment of glutamine to the genetic code. *Science 312*, 1950–1954.
(32) Eigner, E. A., and Loftfield, R. B. (1974) Kinetic techniques for the investigation of amino acid: tRNA ligases (aminoacyl-tRNA synthetases, amino acid activating enzymes). *Methods Enzymol. 29*, 601–619.
(33) Uter, N. T., Gruic-Sovulj, I., and Perona, J. J. (2005) Amino acid-dependent transfer RNA affinity in a class I aminoacyl-tRNA synthetase. *J. Biol. Chem. 280*, 23966–23977.
(34) Nureki, O., Vassylyev, D. G., Katayanagi, K., Shimizu, T., Sekine, S., Kigawa, T., Miyazawa, T., Yokoyama, S., and Morikawa, K. (1995) Architectures of class-defining and specific domains of glutamyl-tRNA synthetase. *Science 267*, 1958–1965.
(35) Ebel, J. P., Giegé, R., Bonnet, J., Kern, D., Befort, N., Bollack, C., Fasiolo, F., Gangloff, J., and Dirheimer, G. (1973) Factors determining the specificity of the tRNA aminoacylation reaction. Non-absolute specificity of tRNA-aminoacyl-tRNA synthetase recognition and particular importance of the maximal velocity. *Biochimie 55*, 547–557.
(36) Giegé, R., Sissler, M., and Florentz, C. (1998) Universal rules and idiosyncratic features in tRNA identity. *Nucleic Acids Res. 26*, 5017–5035.
(37) Alexander, R. W., and Schimmel, P. (2001) Domain-domain communication in aminoacyl-tRNA synthetases. *Prog. Nucleic Acid Res. Mol. Biol. 69*, 317–349.
(38) Banerjee, R., Dubois, D. Y., Gauthier, J., Lin, S. X., Roy, S., and Lapointe, J. (2004) The zinc-binding site of a class I aminoacyl-tRNA synthetase is a SWIM domain that modulates amino acid binding via the tRNA acceptor arm. *Eur. J. Biochem. 271*, 724–733.
(39) Saha, R., Dasgupta, S., Basu, G., and Roy, S. (2009) A chimaeric glutamyl:glutaminyl-tRNA synthetase: implications for evolution. *Biochem. J. 417*, 449–455.
(40) Nooren, I. M., and Thornton, J. M. (2003) Structural characterisation and functional significance of transient protein-protein interactions. *J. Mol. Biol. 325*, 991–1018.
(41) Sekine, S.-i., Shichiri, M., Bernier, S., Chênevert, R., Lapointe, J., and Yokoyama, S. (2006) Structural bases of transfer RNA-dependent amino acid recognition and activation by glutamyl-tRNA synthetase. *Structure 14*, 1791–1799.
(42) Liu, J., Gagnon, Y., Gauthier, J., Furenlid, L., L'Heureux, P. J., Auger, M., Nureki, O., Yokoyama, S., and Lapointe, J. (1995) The zinc-binding site of *Escherichia coli* glutamyl-tRNA synthetase is located in the acceptor-binding domain. Studies by extended x-ray absorption fine structure, molecular modeling, and site-directed mutagenesis. *J. Biol. Chem. 270*, 15162–15169.
(43) Schimmel, P., Giegé, R., Moras, D., and Yokoyama, S. (1993) An operational RNA code for amino acids and possible relationship to genetic code. *Proc. Natl. Acad. Sci. U.S.A. 90*, 8763–8768.
(44) Sherlin, L. D., and Perona, J. J. (2003) tRNA-dependent active site assembly in a class I aminoacyl-tRNA synthetase. *Structure 11*, 591–603.
(45) Sherman, J. M., Rogers, M. J., and Soll, D. (1995) Recognition in the glutamine tRNA system: from structure to function, in tRNA: Structure, Biosynthesis, and Function (Soll, D., and RajBhandary, U. L., Eds.) pp 395−409, American Society for Microbiology, Washington, DC.
(46) Ibba, M., Hong, K. W., and Soll, D. (1996) Glutaminyl-tRNA synthetase: from genetics to molecular recognition. *Genes Cells 1*, 421–427.
(47) Giegé, R., and Frugier, M. (2003) Transfer RNA structure and identity, in Translation Mechanisms (Lapointe, J., and Brakier-Gingras, L., Eds.) pp 1−24, Eurekah.com/Landes Bioscience, Georgetown, TX.
(48) Giegé, R., Lapointe, J. (2008) Transfer RNA aminoacylation and modified nucleosides, in DNA and RNA Modification Enzymes: Comparative Structure, Mechanism, Function, Cellular Interactions and Evolution (Grosjean, H., Ed.) Chapter 31, Eurekah.com/Landes Bioscience, Georgetown, TX.
(49) Rogers, M. J., Adachi, T., Inokuchi, H., and Soll, D. (1994) Functional communication in the recognition of tRNA by *Escherichia coli* glutaminyl-tRNA synthetase. *Proc. Natl. Acad. Sci. U.S.A. 91*, 291–295.
(50) Weygand-Đurašević, I., Rogers, M. J., and Soll, D. (1994) Connecting anticodon recognition with the active site of *Escherichia coli* glutaminyl-tRNA synthetase. *J. Mol. Biol. 240*, 111–118.
(51) Wright, D. J., Martinis, S. A., Jahn, M., Soll, D., and Schimmel, P. (1993) Acceptor stem and anticodon RNA hairpin helix interactions with glutamine tRNA synthetase. *Biochimie 75*, 1041–1049.
(52) Yaremchuk, A., Cusack, S., and Tukalo, M. (2000) Crystal structure of a eukaryote/archaeon-like prolyl-tRNA synthetase and its complex with $tRNA^{Pro}$ (CGG). *EMBO J. 19*, 4745–4758.
(53) Miller, G. P., and Benkovic, S. J. (1998) Stretching exercises-flexibility in dihydrofolate reductase catalysis. *Chem. Biol. 5*, R105–R113.
(54) Daniel, R. M., Dunn, R. V., Finney, J. L., and Smith, J. C. (2003) The role of dynamics in enzyme activity. *Annu. Rev. Biophys. Biomol. Struct. 32*, 69–92.
(55) Fersht, A. (1999) Structure and Mechanism in Protein Science. A Guide to Enzyme Catalysis and Protein Folding , 1st ed., W. H. Freeman, New York.
(56) Freist, W., Gauss, D. H., Soll, D., and Lapointe, J. (1997) Glutamyl-tRNA sythetase. *Biol. Chem. 378*, 1313–1329.
(57) Sugiura, I., Nureki, O., Ugaji-Yoshikawa, Y., Kuwabara, S., Shimada, A., Tateno, M., Lorber, B., Giegé, R., Moras, D., Yokoyama, S., and Konno, M. (2000) The 2.0 Å crystal structure of *Thermus thermophilus* methionyl-tRNA synthetase reveals two RNA-binding modules. *Struct. Folding Des. 8*, 197–208.